

МІНІСТЕРСТВО ОСВІТИ І НАУКИ УКРАЇНИ
НАЦІОНАЛЬНИЙ АВІАЦІЙНИЙ УНІВЕРСИТЕТ
ФАКУЛЬТЕТ АЕРОНАВІГАЦІЇ, ЕЛЕКТРОНІКИ ТА ТЕЛЕКОМУНІКАЦІЙ
КАФЕДРА АЕРОКОСМІЧНИХ СИСТЕМ УПРАВЛІННЯ

ДОПУСТИТИ ДО ЗАХИСТУ

Завідувач кафедри

_____ Юрій МЕЛЬНИК

«_____» _____ 2024 р.

КВАЛІФІКАЦІЙНА РОБОТА

(ПОЯСНЮВАЛЬНА ЗАПИСКА)

ВИПУСКНИКА ОСВІТНЬОГО СТУПЕНЯ
«БАКАЛАВР»

Тема: «Адаптивна система автоматичного управління безпілотним літальним апаратом»

Виконавець: студент групи СУ-404 Чайка Дмитро Миколайович

Керівник: завідувач кафедри, Мельник Юрій Віталійович

Нормоконтролер: _____ Микола Дивнич

Київ 2024

MINISTRY OF EDUCATION AND SCIENCE OF UKRAINE
NATIONAL AVIATION UNIVERSITY
FACULTY OF AIR NAVIGATION, ELECTRONICS AND TELECOMMUNICATIONS
AEROSPACE CONTROL SYSTEMS DEPARTMENT

APPROVED FOR DEFENCE

Head of the Department

_____ Yuri MELNYK

“ _____ ” _____ 2024

QUALIFICATION PAPER

(EXPLANATORY NOTE)

FOR THE ACADEMIC DEGREE OF BACHELOR

Title: “Adaptive system of automatic control of an unmanned aerial vehicle”

Submitted by: student of group CS-404 Chaika Dmytro Mykolayovych

Supervisor: Head of the Department Yuri MELNYK

Standards inspector: _____ Mykola DYVNYCH

Kyiv 2024

НАЦІОНАЛЬНИЙ АВІАЦІЙНИЙ УНІВЕРСИТЕТ

Факультет аеронавігації, електроніки та телекомунікацій

Кафедра аерокосмічних систем управління

Спеціальність: 151 «Автоматизація та комп'ютерно-інтегровані технології»

ЗАТВЕРДЖУЮ

Завідувач кафедри

_____ Юрій МЕЛЬНИК

«_____» _____ 2024 р.

ЗАВДАННЯ

на виконання кваліфікаційної роботи
Чайки Дмитра Миколайовича

1. Тема кваліфікаційної роботи «Адаптивна система автоматичного управління безпілотним літальним апаратом» затверджена наказом ректора від «01» квітня 2024 р. № 511/ст.
2. Термін виконання роботи: з 13.05.2024 по 16.06.2024.
3. Вихідні дані роботи: дослідити аналітичний огляд літературних джерел та статей з тематики диплому; наведений точний опис літального апарату, викладені принципи його роботи.
4. Зміст пояснювальної записки:
5. Перелік обов'язкового ілюстративного матеріалу:

6. Календарний план-графік

№ пор.	Завдання	Термін виконання	Відмітка про виконання
1	Отримання завдання	06.03.24	
2	Уточнення с приводу літератури	07.05.24	
3	Аналіз літературних джерел	12.05.24	
4	Розробка змісту дипломної роботи	14.05.24	
5	Вступ	17.05.24	
6			
7			
8			
9			
10			

7. Дата видачі завдання: «13» травня 2024 р.

Керівник кваліфікаційної роботи

(підпис керівника)

Юрій МЕЛЬНИК

Завдання прийняв до виконання

(підпис випускника)

Чайка Дмитро

NATIONAL AVIATION UNIVERSITY

Faculty of Air Navigation, Electronics and Telecommunications

Aerospace Control Systems Department

Specialty: 151 “Automation and Computer-integrated Technologies”

APPROVED BY

Head of the Department

_____ Yurii MELNYK

“ _____ ” _____ 2024

Qualification Paper Assignment for Graduate Student

Chaika Dmytro Mykolayovych

1. The qualification paper title “Adaptive system of automatic control of an unmanned aerial vehicle” was approved by the Rector’s order of “ 01 ” April 2024 № 511/CT.
2. The paper to be completed between: 13.05.2024 and 16.06.2024
3. Initial data for the paper: research an analytical review of literary sources and articles on the subject of the diploma, an accurate description of the aircraft is given, the principles of its operation are outlined.
4. The content of the explanatory note:
5. The list of mandatory illustrations:

6. Timetable

№	Assignment	Dates of completion	Completion mark
1	Receiving the task	06.03.24	
2	Clarification about the literature	07.05.24	
3	Analysis of literary sources	12.05.24	
4	Development of the content of the thesis	14.05.24	
5			
6			
7			
8			
9			
10			

7. Assignment issue date: “13” May 2024

Qualification paper supervisor _____
(the supervisor's signature)

Yurii MELNYK

Issued task accepted _____
(the graduate student's signature)

Chaika Dmytro

ESSAY

The text part of the work:60 pages.

Object of research is a four-engine aircraft

The subject of research is the aircraft control system

The purpose of the work is to develop an aircraft control system that allows stabilization along the main axes of rotation: roll, pitch and yaw.

Research methods are the follows Scientific articles, publications and other sources related to unmanned aerial vehicles were analyzed. This method made it possible to obtain the necessary theoretical knowledge about the development of control systems and stabilization of aircraft.

Abbreviation: PID it's a proportional-integral-differential regulator, AU is Automatic control, IS means integrated system, CS is control system

CONTENT

Introduction.....	9
Section 1. Multi-rotor flight apparatus.....	10
1.1 Definition and principle of operation.....	
1.2 The history of the development of four-engine aircraft.....	
1.3 Aircraft components.....	
Section 2. Simulation.....	
Section 3.	
Section 4.	

Introduction

Section 1

Multicopter Aircraft (drones)

In this section will be explained what it is, how it works and will be reviewed literature that shows history of development of drones of similar type.

1.1 types of drones and working principle

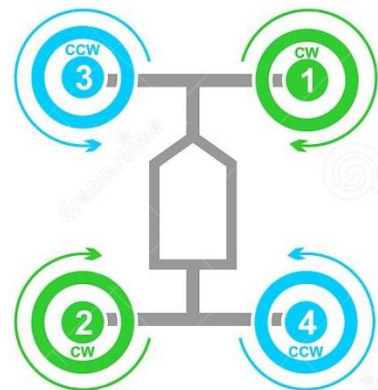
Multicopter- unmanned aerial vehicle which have two or more rotors that generate lift force.

One of the most common types of multicopter is quadcopter, its a multicopter with four propellers usually placed in a square formation. Control of quadcopter is interesting and at the same time difficult problem because this rotors have 6 degrees of freedom but only four inputs.

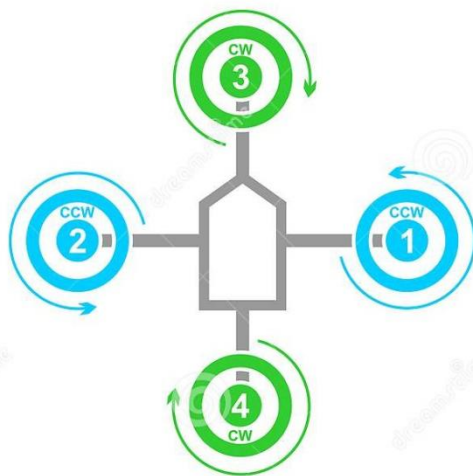
Here on this picture shown most popular placement of rotors on quadcopters



QUAD X



QUAD H



QUAD+



QUAD V

But mostly used models QuadX and Quad+ they are quite easy at usage and construction. Model X allows to gain more speed than + model because of placement of its rotors, In + model only one of them is responsible for movement in the horizontal direction while X have two of them.

At this work speed doesn't matter so we will be using model + to complete this task easier, in this model only one pair of rotors used in changing position of the copter in relation of its axes.

Each engine with a supporting screw is located on the vertices of an imaginary square, so each pair of diagonally placed screws has opposite rotation direction to other pair. At this placement the torque created by screws is compensated, if we make all screws turn in one side than our quadcopter will start turning to opposite direction.

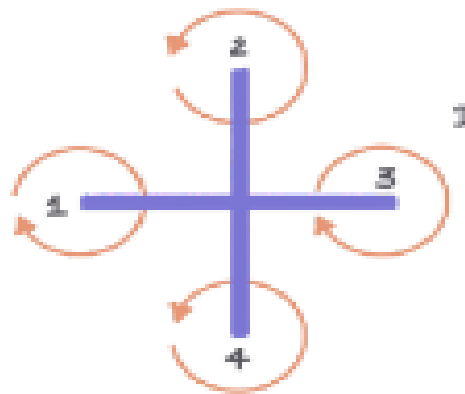
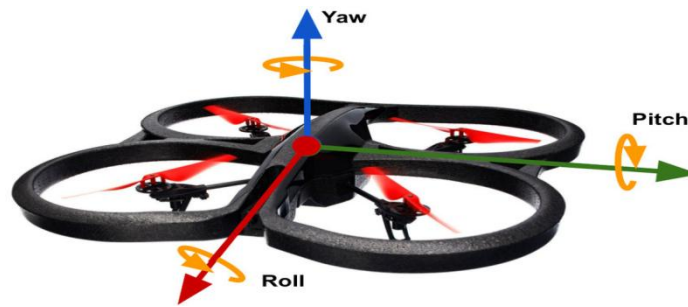


fig.2. Direction of engine rotation

Position of quadcopter relative to connected to it coordinate system is determine by angles, to be more precise there are three angles: roll, pitch and yaw.

- roll - angle of rotation of the longitudinal axis;
- pitch - angle between the longitudinal axis of the aircraft and the horizontal plane;
- yaw - angle relative to the vertical axis.



Quadcopter can fly in four modes such as: roll, pitch, yaw and to this also add hover.

To gain altitude all engines should increase power by the same amount.

Control of the roll and pitch angle can be carried out by the increase of the power of one engines while decreasing it in the opposite one. While xis roll and pitch depend on the initial choice of direction of movement.

Yaw angle control is carried out by adding power to the engines, that rotates in the opposite direction to other two engines the power of which will be decreased. At the same time, altitude gain is not performed, since total power of the engines does not change

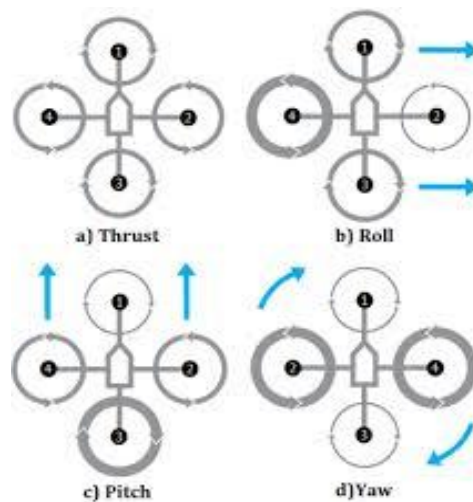


fig.3. Roll, pitch and yaw control

Hover mode is used when thrust of engine will balance the force of gravity acting on the quadcopter, while roll and pitch angles must be close to zero.

For determination of angles of quadcopter it has installed on-board control system, which is equipped with position sensors. It's main task is tracking orientation of the device in space and stabilizing its flight by changing speed of rotation of corresponding screws.

1.2 The history of the development of four-engine aircraft

The first four rotor aircraft shown themselves early starting from 1907. August this year first aircraft with such design lifted off the ground by two feet. It was created by Louis Charles Breguet, it was lacking at stability and control and its motion was limited by four tethers

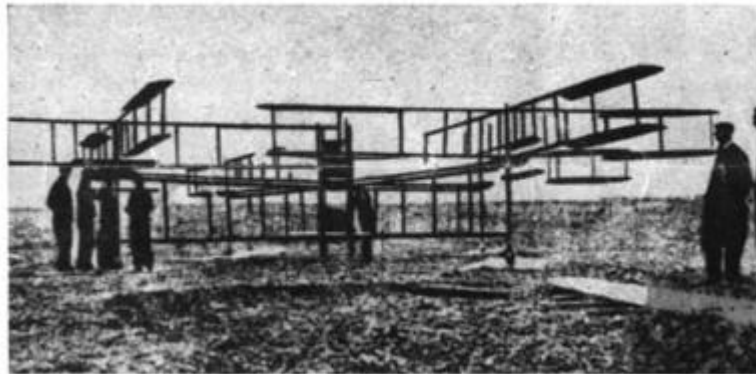


fig.4. Breguet-Richet Gyroplane No. 1

In 1921 more successful program was funded in USA. In addition to four main rotors they used two propellers for control of direction, and two more placed above engine to help lift it higher and cool engine. By conducting over 100 test flights Dr. George de Bothezat's model proved to be more stable while flying with three men which provided an asymmetric weight distribution and could rise to maximum height of 1.8 meters and be in the air for 1 minute and 42 seconds. He was provided with additional funding but when test didn't provide needed result program was canceled in 1923.



fig.5. De Bothezat's quadrotor

Later, on April 1924 Etienne Oehmichen broke existing record for helicopter flight by lifting by 360m and flying for 525m. He went to fly over thousand test flights using his model of quadrotor with additional propellers for control.

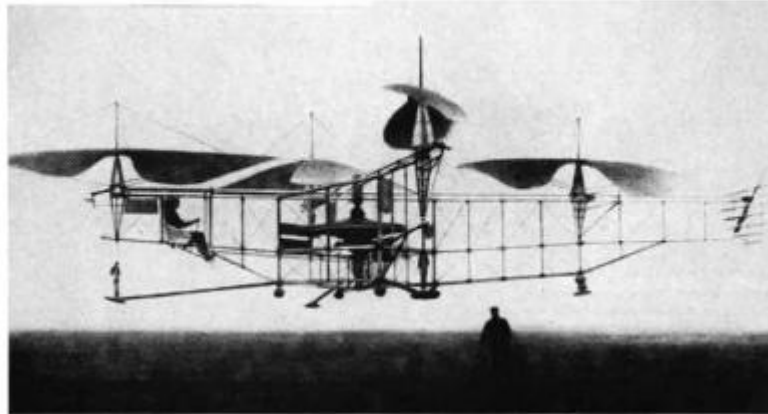


fig.6. Oemichen's record setting quadrotor

Paisecki Aircraft Corporation managed to build quadrotor UAV that met requirements for a weapons delivery platform, launched from naval destroyers. In 1958 this model PA-4 Sea Bat achieved hover and maintained reached attitude in tethered flight using differential tilt for control.

In the last years technology evolved to such extent that it is possible to build much better quadcopters and different types, smaller ones which can serve both professional and recreational purpose and big ones mainly used in army for transporting troops

1.3 Components of aircraft

First component will be circuit board arduino model Mega2560

Arduino - its a open platform which helps with electronics it has its own circuit boards to work with them it has its own language and software. The most popular way of using this platform is the creation with its help small automatic projects. It became popular because of its low, comparing to others, cost and its easy to use.

This model is quite easy to use and have quite enough inputs and outputs. Here characteristics of this board and picture of it (fig.7).

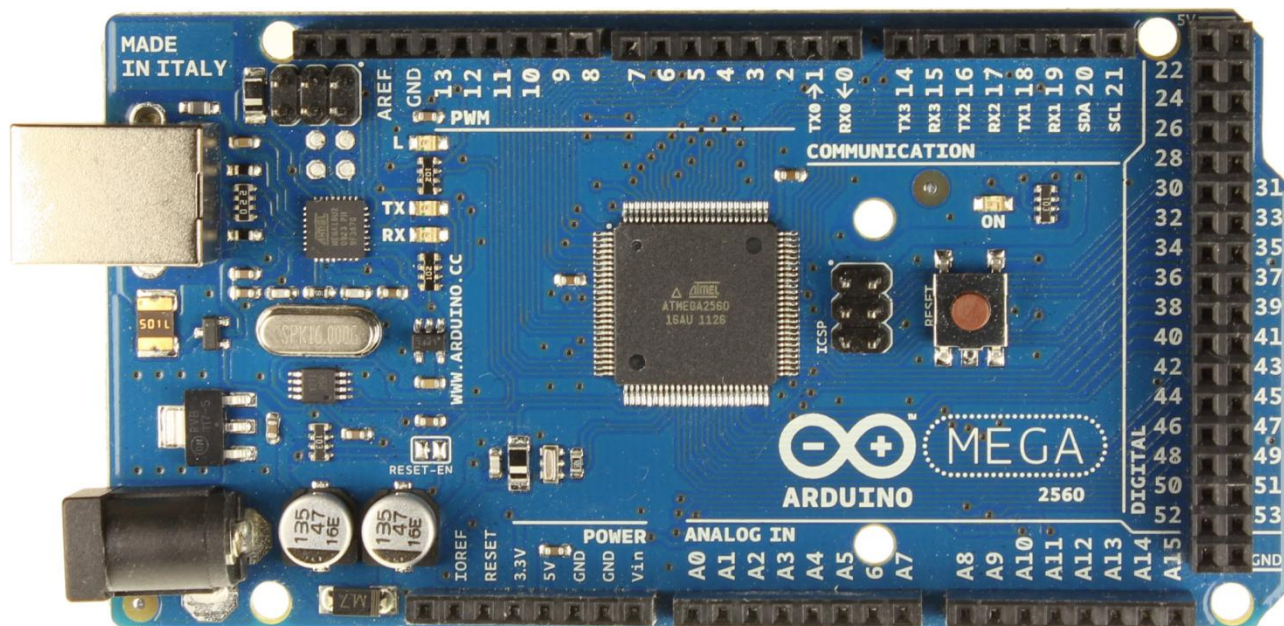


fig.7. Mega 2560

Hardware serial ports	4
Operating Voltage	5V
Input Voltage(recommended)	7-12V
Input Voltage(limits)	6-20V
DC Current per Pin	40mA
Digital pins	54
Analog Input pins	16
Flash Memory	256 KB(8 used by bootloader)
SRAM	8 KB
EEPROM	4 KB

Second component is module GY-88

This part is used for determination of the position of the aircraft in space it includes 3-axis gyroscope, 3-axis accelerometer and DMP(Digital Motion Processor) and have 3 inbuilt components:

1. MPU 6050-motion sensor
2. HMC5883L-three-axis digital magnetometer
3. BMP085-barometer pressure sensor

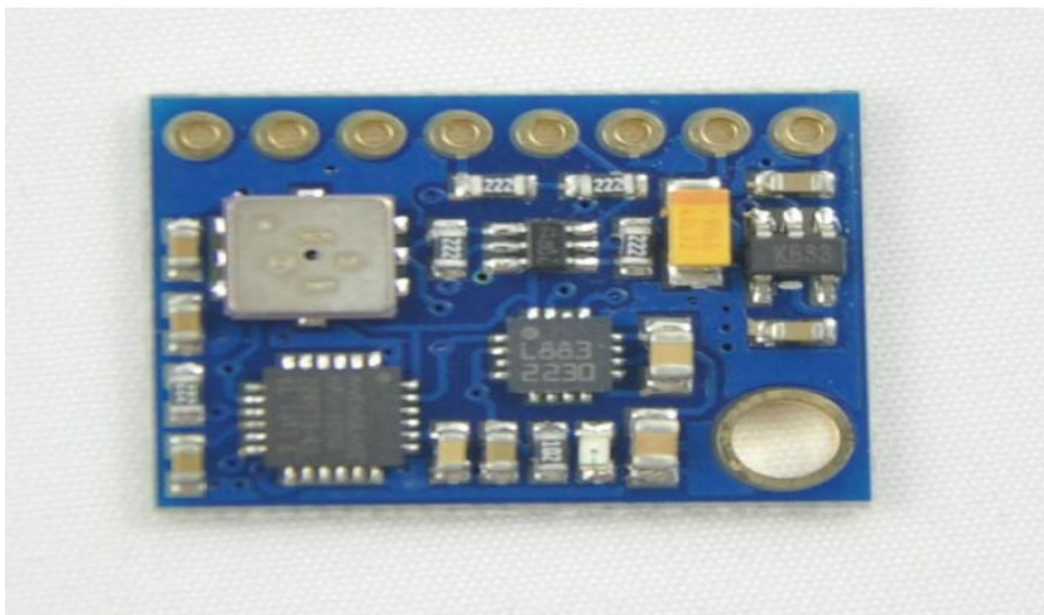


fig.8. module GY-88

MPU-6050 is a popular accelerometer and at the same time gyro with six axes of sensing and 16-bit measurements. Also it has included ability to choose measurement accuracy for gyroscope its from ± 250 to ± 2000 each step is double of previous, and for accelerometer from $\pm 2g$ to $\pm 16g$.

By experimenting was established that to calculate the angle of rotation, magnetometer indicators needed, because during calculation around vertical axis of the aircraft appears a strong drift of values with time.

So for magnetometer module HMC5883L it allows to estimation of the voltage vector of earth magnetic field and it has accuracy settings too: ± 0.88 , ± 1.3 , ± 1.9 , ± 2.5 , ± 4.0 , ± 4.7 , ± 5.6 ,

±8.1G and its partially used as a compass.

BMP085 pressure sensor has pressure sensing range from 300 to 1100 hPa and used for estimation of the altitude also it has different modes:

1. standard mode with accuracy 0.5m
2. ultra-high mode with accuracy 0.25m
3. using filter accuracy is equal 0.1m

Module GY-88 also has the following contacts:

- Vin-for power supply 5B;
- 3,3V-for voltage output;
- GND-for earth;
- SCL-data bus of I2C interface;
- SDA-I2C interface synchronization bus;
- M_DRDY-output for HMC5883L;
- G_ADO-selection of one of two I2C addresses for MPU-6050;
- G_INT-interrupt pin for MPU-6050

As an engine was used three-phased brushless DC motors. They consist of a rotor with permanent magnets and stator with windings. Stator consists of three components case, core and copper winding. By the number of winding determined the number of phases of the motor. Mostly used three phased ones but to start motor its sufficient to have only 2 phases.

The rotor consists of permanent magnets and has from two to eight pairs of poles with alternating north and south poles.

In a three-phase motor, there are six possible connections of motor windings to the power source, as at any given time voltage is supplied to only two windings. This allows creating a magnetic field with rotating steps of 60 degrees with each switch.

Let's list the main advantages of brushless motors compared to their counterparts:

- Precision and high speed operation;

- Wide range of speed variation;
- Motor efficiency over 90%;
- High reliability due to the absence of sliding electrical contacts;
- Low motor overheating.

We need A2212 motors for work.

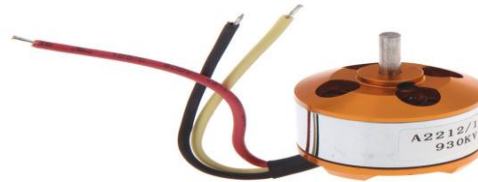


fig.9. A2212 motor

The motor has the following characteristics:

Stator diameter	22mm
Stator length	12mm
RPM per volt	1000
Maximum efficiency	80%
Maximum efficiency at a current of 10 A	>75%
No-load current	0.5 A
Dimensions	27.5x30mm
Shaft diameter	3.17mm
Weight	47g

According to tests, one motor at its peak load can lift payloads weighing up to 800 grams. With a quadcopter weight of 0.96 kg, the selected motors provide sufficient lifting force, allowing for future payload additions.

Motor Speed Controllers

The Electronic Speed Controller (ESC) allows smooth variation of the power supplied to the connected brushless motor based on the input control signal.

Power control, and consequently motor speed control, is achieved through phase-pulse modulation, meaning through pulses of equal duration spread over time intervals of encoded power values. The standard encoded signal range for controllers is between 1000-2000 microseconds.

To change the direction of the motor rotation, it is sufficient to swap the wires of any two phases.

The project utilized Hobbysky brand speed controllers, which come with the motors.

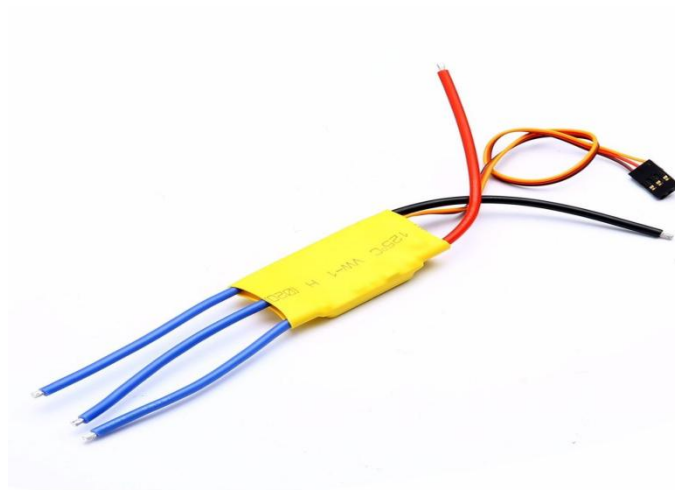


fig.10. Hobbysky speed controllers

Radio Communication

For manual control of the aircraft or transmitting commands remotely, we will use the

WFT07 remote control, with the following characteristics:

- 7 control channels;
- Data transmission frequency: 2.4 GHz;
- Range up to 800 meters;
- Power supply voltage: 3.7-6V.



fig.11. Remote controller WFT07

The WFR07S model was chosen as the receiver, which comes with the remote control.



fig.12. Receiver WFR07S

Propellers

Standard plastic propellers with dimensions of 10x4.5 will be used.



fig.13. propellers

Frame

The HJ450 frame made of plastic was used for the project. It has high strength, light weight, and enough space for all other components of the aircraft.

It has following features:

- weight-282g;
- distance between motors diagonally-450mm.



fig.14. frame HJ450

Battery

The HRB LiPo battery will be used as the power source for the motors and all internal

electronics:

- voltage: 11.1V
- capacity:2200 mAh
- operating current:66A
- number of cells: from 3 to 3.7V;
- weight:182g
- dimensions 102x34x22mm



fig.15. Battery HRB

Section 2

2.1 MATHEMATICAL MODELING

Coordinate Systems Various coordinate systems are used to determine the position in space and describe the motion of the quadcopter: inertial, earth-fixed, and moving coordinate systems.

The normal earth-fixed coordinate system is rigidly attached to the Earth and is considered inertial. The origin of such a system is located on the surface of the Earth at an arbitrary point. The axis is tangent to the surface of the Earth at that point. The axis perpendicular to the surface of the Earth is directed upwards along the local vertical. The axis perpendicular to the vertical plane forms a right-handed Cartesian coordinate system.

The moving coordinate system coincides with the axes of the quadcopter. Its origin coincides with the center of gravity of the aircraft, and the axes are rotated by angles of roll, pitch, and yaw from the axes of the chosen fixed coordinate system.

As the fixed coordinate system, we will use the NED (North-East-Down) system, which represents a three-dimensional Cartesian coordinate system with axes directed to the north, east, and down, perpendicular to each other.

Then the axes of the moving coordinate system of the aircraft will be oriented as shown in Fig. 16.

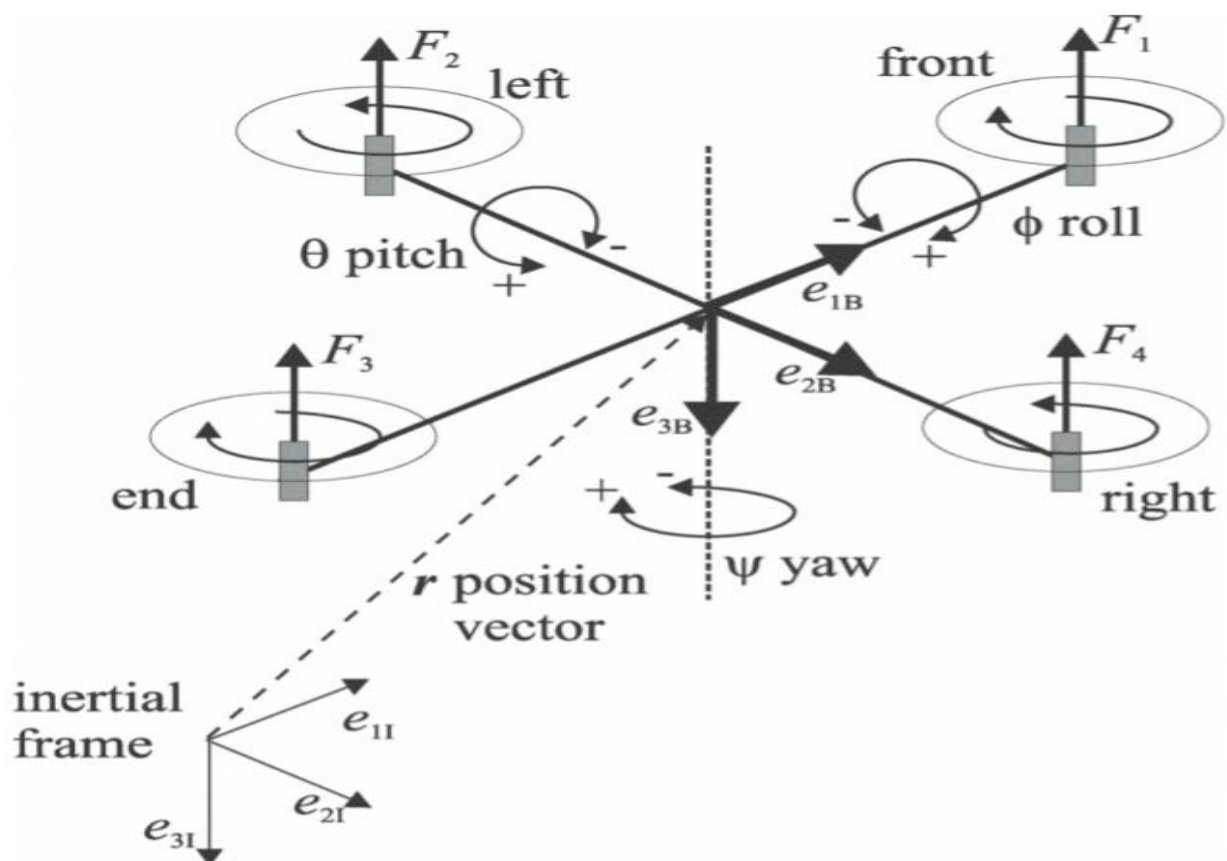


fig.16. Quadcopter coordinate system

Let's denote the roll, pitch, and yaw angles as ϕ , θ , and ψ , respectively. The angular velocities around the roll, pitch, and yaw axes are denoted as p , q , and r . The linear velocities along the axes of the fixed coordinate system of the aircraft are denoted as u , v , and w . The lift forces acting on each propeller are denoted as F_i . To transition from the moving coordinate system to the fixed one, we will use rotation matrices.

A 3x3 rotation matrix is a transformation matrix for a three-dimensional position vector in Euclidean space, which converts the coordinates of a vector from the attached coordinate system to the absolute coordinate system.

Rotation matrix around the axis by angle θ has the form:

$$R_z(\theta) = \begin{pmatrix} \cos(\theta) & \sin(\theta) & 0 \\ -\sin(\theta) & \cos(\theta) & 0 \\ 0 & 0 & 1 \end{pmatrix}$$

Rotation matrix around the axis by angle ϕ has the form:

$$R_x(\phi) = \begin{pmatrix} 1 & 0 & 0 \\ 0 & \cos(\phi) & \sin(\phi) \\ 0 & -\sin(\phi) & \cos(\phi) \end{pmatrix}$$

Rotation matrix around the axis by angle ψ has the form:

$$R_y(\psi) = \begin{pmatrix} \cos(\psi) & 0 & -\sin(\psi) \\ 0 & 1 & 0 \\ \sin(\psi) & 0 & \cos(\psi) \end{pmatrix}$$

The sequence of rotations around the z-y-x axes is described by the general rotation matrix $R_{zyx} = R_z(\psi) \cdot R_y(\theta) \cdot R_x(\phi)$. This matrix describes the transition from the moving coordinate system of the aircraft to the chosen fixed coordinate system.

$$D = \begin{bmatrix} \cos(\theta)\cos(\psi) & \cos(\theta)\sin(\psi) & -\sin(\theta) \\ \sin(\phi)\sin(\theta)\cos(\psi)\cos(\phi)\sin(\psi) & \sin(\phi)\sin(\theta)\sin(\psi)\cos(\phi)\cos(\psi) & \sin(\phi)\cos(\psi) \\ \cos(\phi)\sin(\theta)\cos(\psi)+\sin(\phi)\sin(\psi) & \cos(\phi)\sin(\theta)\sin(\psi)-\sin(\phi)\cos(\psi) & \cos(\phi)\cos(\theta) \end{bmatrix}$$

2.2 Equations of Motion

The following state equation relates the change in the position of the quadcopter in a fixed coordinate system to the change in linear velocities in the moving system:

$$\begin{bmatrix} \dot{x} \\ \dot{y} \\ \dot{z} \end{bmatrix} = D^{-1} \begin{bmatrix} u \\ v \\ w \end{bmatrix}$$

The transition from angular velocities in the fixed coordinate system to the moving one is

accomplished using the matrix E:

$$\begin{bmatrix} q \\ r \end{bmatrix} = E \begin{bmatrix} 0 \\ \dot{\tau} \end{bmatrix}$$

In this case:

$$E = \begin{bmatrix} 1 & 0 & -\sin(0) \\ 0 & \cos(\tau) & \sin(\tau)\cos(0) \\ 0 & -\sin(\tau) & \cos(\tau)\cos(0) \end{bmatrix}$$

Then, the inverse transition is described by the expression:

$$\begin{bmatrix} 0 \\ \dot{\tau} \end{bmatrix} = E^{-1} \begin{bmatrix} q \\ r \end{bmatrix}$$

2.2.1 Linear Acceleration

Let's apply Newton's second law:

$$F = m * V$$

where

m is the mass of the quadcopter;

V - its velocity vector.

Since the vector V, besides changing its components, can also rotate, we need to take its total derivative:

$$F = m * \dot{V} + \omega * m * V$$

where ω - the vector of angular velocities of the aircraft.

Then we obtain:

$$\begin{bmatrix} F_x \\ [F_y] \\ F_z \end{bmatrix} = m \begin{bmatrix} u' \\ v' \\ w' \end{bmatrix} + m \begin{bmatrix} p \\ q \\ r \end{bmatrix} \begin{bmatrix} u \\ v \\ w \end{bmatrix}$$

After multiplying matrices and simplifying similar terms:

$$\begin{bmatrix} F_x \\ [F_y] \\ F_z \end{bmatrix} = m \begin{bmatrix} u' \\ v' \\ w' \end{bmatrix} + m \begin{bmatrix} p \\ q \\ r \end{bmatrix} \begin{bmatrix} u \\ v \\ w \end{bmatrix}$$

If we neglect aerodynamic forces, then the external forces acting on the quadcopter will be:

- Thrust from the propellers (T)
- Weight force (W).

The thrust from the propellers is always directed along the axis, while the weight force has its projections depending on the position of the aircraft. Let's substitute the external forces instead of F:

$$\begin{bmatrix} W_x \\ [W_y] \\ W_z - T \end{bmatrix} = m \begin{bmatrix} u' \\ v' \\ w' \end{bmatrix} + m \begin{bmatrix} p \\ q \\ r \end{bmatrix} \begin{bmatrix} u \\ v \\ w \end{bmatrix}$$

However, in the fixed coordinate system, the weight force is always directed along the axis. Therefore, using the rotation matrix, we can rewrite the previously obtained equation as follows:

$$\begin{bmatrix} 0 \\ [0] \\ m \cdot q \end{bmatrix} - \begin{bmatrix} 0 \\ [0] \\ T \end{bmatrix} = m \begin{bmatrix} u' \\ v' \\ w' \end{bmatrix} + m \begin{bmatrix} p \\ q \\ r \end{bmatrix} \begin{bmatrix} u \\ v \\ w \end{bmatrix}$$

Transforming further, we obtain a system of three equations:

$$u' = r \cdot v - q \cdot w - g \cdot \sin(\theta)$$

$$v' = p \cdot v - r \cdot u + g \cdot \cos(\theta) \sin(\phi)$$

$$w' = q * u - p * v + g * \cos(\phi) \cos(0) - T/m$$

If we don't consider motor dynamics, the thrust is proportional to the sum of the squares of the angular velocities of the propellers:

$$T = b(f_1^2 + f_2^2 + f_3^2 + f_4^2)$$

here f means speed of each engine

b-the thrust coefficient.

Let's substitute the equations described above and obtain the set of equations:

$$u' = r * v - q * w - g * \sin(0)$$

$$v' = p * v - r * u + g * \cos(0) \sin(\phi)$$

$$w' = q * u - p * v + g * \cos(\phi) \cos(0) - \frac{b}{m}(f_1^2 + f_2^2 + f_3^2 + f_4^2)$$

2.2.2 Angular Acceleration

The quadcopter's angular momentum will change when an external torque is applied:

$$M = H'$$

Where H is the angular momentum

M is the external torque.

Since the angular momentum is capable of changing its direction, it is necessary to take its total derivative:

$$M = H' + \omega * H$$

The angular momentum is defined by the equation:

$$H=I*\omega$$

In this case I- moment of inertia

ω is the vector of angular velocities of rotation.

Since the quadcopter is symmetric with respect to its planes, and the axes of rotation coincide with the principal axes of inertia, the moment of the inertia tensor is equal to:

$$I = \begin{bmatrix} I_x & 0 & 0 \\ 0 & I_y & 0 \\ 0 & 0 & I_z \end{bmatrix}$$

I_x , I_y , and I_z are the moments of inertia of the quadcopter with respect to its axes. Substituting the corresponding formulas, we obtain:

$$M=I*\omega + \omega*I*\omega$$

After transformation:

$$M_x = p' * I_x + q * r (I_z - I_y)$$

$$M_y = q' * I_y + p * r (I_x - I_z)$$

$$M_z = r' * I_z + p * q (I_y - I_x)$$

So because the planes are symmetric. $I_x=I_y$, then:

$$M_x = p' * I_x + q * r (I_z - I_y)$$

$$M_y = q' * I_y + p * r (I_x - I_z)$$

$$M_z = r' * I_z$$

External torques are caused by the thrust and drag of the propellers. Neglecting inertia and aerodynamic torques of the propellers, they can be written as:

$$M_x = l \cdot b(f_{i_2}^2 - f_{i_4}^2)$$

$$M_y = l \cdot b(f_{i_1}^2 - f_{i_3}^2)$$

$$M_z = d(f_{i_2}^2 + f_{i_4}^2 - f_{i_1}^2 - f_{i_3}^2)$$

Where d is the coefficient of frontal drag of the propellers, and l is the distance from the propeller to the center of gravity of the quadcopter. Then we get:

$$p' = \frac{l \cdot b}{I_x} (f_{i_2}^2 - f_{i_4}^2) - q \cdot r \frac{l_z \cdot l_y}{I_x}$$

$$q' = \frac{l \cdot b}{I_y} (f_{i_1}^2 - f_{i_3}^2) - p \cdot r \frac{l_x \cdot l_z}{I_y}$$

$$r' = \frac{d}{I_z} (f_{i_2}^2 + f_{i_4}^2 - f_{i_1}^2 - f_{i_3}^2)$$

The system of state equations describes the dynamics of the quadcopter and its motion equations.

2.2.3 Gyroscopic Effect of Propellers

A gyroscope is a massive symmetrical body that rotates rapidly about its symmetry axis.

The gyroscopic effect manifests itself in that if a torque is applied to a gyroscope that is rotating, which tends to turn it around an axis perpendicular to the gyroscope's rotation axis, it will begin to rotate about a third axis perpendicular to the first two.

Taking into account the gyroscopic effect, we obtain:

$$\begin{aligned}
M_x &= \dot{p} \cdot I_x + q \cdot r(I_z - I_y) + \dot{H}_x + H_z \cdot q - H_y \cdot r \\
M_y &= \dot{q} \cdot I_y + p \cdot r(I_x - I_z) + \dot{H}_y + H_x \cdot r - H_z \cdot p \\
M_z &= \dot{r} \cdot I_z + \dot{H}_z + H_y \cdot p - H_x \cdot q
\end{aligned}$$

Where H_x, H_y, H_z are the total angular moments of bodies rotating around axes.

$$\begin{aligned}
H_x &= \sum_{i=1}^4 I_{xi} \cdot \omega_{xi} \\
H_y &= \sum_{i=1}^4 I_{yi} \cdot \omega_{yi} \\
H_z &= \sum_{i=1}^4 I_{zi} \cdot \omega_{zi}
\end{aligned}$$

Angular velocities of the motors are present only along the axis, so we get:

$$\begin{aligned}
M_x &= p' \cdot I_x + q \cdot r(I_z - I_y) + H_z \cdot q \\
M_y &= q' \cdot I_y + p \cdot r(I_x - I_z) - H_z \cdot p \\
M_z &= r' \cdot I_z + H_z'
\end{aligned}$$

Then the set of equations for the angular velocities of the quadcopter, taking into account the gyroscopic effects of the propellers, will be written as:

$$\begin{aligned}
\dot{p} &= \frac{l \cdot b}{I_x} (\omega_2^2 - \omega_4^2) - q \cdot r \frac{I_z - I_y}{I_x} + \frac{H_z}{I_x} q \\
\dot{q} &= \frac{l \cdot b}{I_y} (\omega_1^2 - \omega_3^2) - p \cdot r \frac{I_x - I_z}{I_y} - \frac{H_z}{I_y} p \\
\dot{r} &= \frac{d}{I_z} (\omega_2^2 + \omega_4^2 - \omega_1^2 - \omega_3^2) + \frac{H_z}{I_z}
\end{aligned}$$

2.3 Quadcopter Identification

2.3.1 Transfer Function of Motors Schematically, a brushless motor can be represented as shown in Fig. 17.

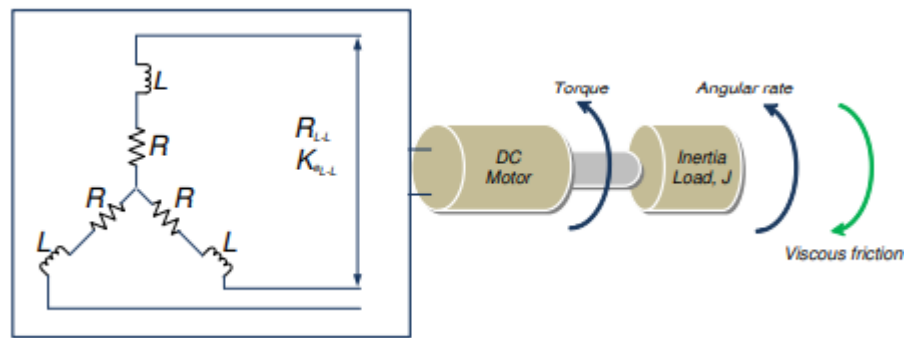


fig.17.Brushless DC motor schematic diagram

where R is the resistance of the winding

L is the inductance.

The transfer function of the motor is represented by the expression:

$$G(s) = \frac{1}{K_e} \frac{1}{r_m * r_e * s^2 + r_m * s + 1}$$

r_m equal $\frac{3 * R}{K_e * K_L}$ and is the mechanical constant

r_e - the electrical constant

The electrical torque is determined by the formula:

$$K_e = \frac{K_{(e*(L-L))}}{\sqrt{3}}$$

The torque constant can be expressed as K_e :

$$K_t = 0,0605 * K_e$$

Since the manufacturer of the selected motors did not provide information about their electrical characteristics, and specialized equipment is needed to find them independently, it was decided to find the transfer function experimentally. For this purpose, a control signal was applied to the motor at rest to accelerate it to maximum speed. To measure the motor's rotation frequency, an optocoupler was used (Fig. 18), which consists of an optical emitter and a phototransistor.

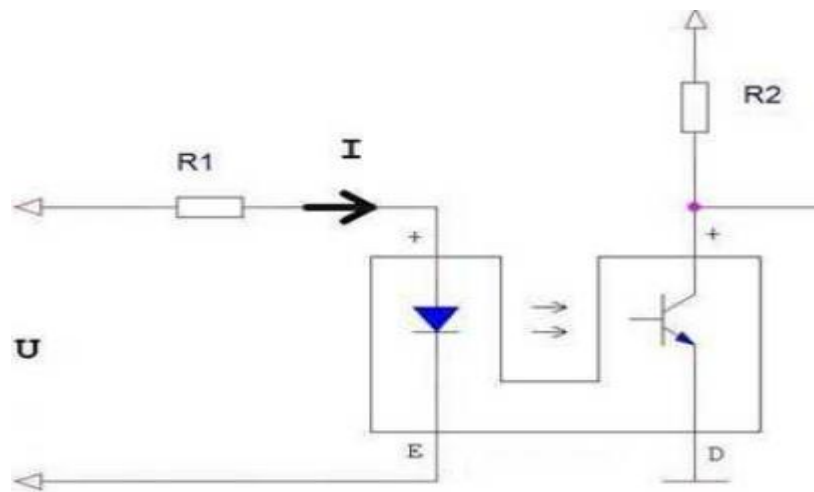


fig.18.

The obtained data were then analyzed in Matlab using the ident module, and the transfer function was obtained in this way.

Resistor R1 limits the LED current to 25 mA, and resistor R2 limits the collector current of the output transistor to 5 mA.

The light flux from the emitter falls on the phototransistor and opens it, resulting in a logic 0 at the output. When there is an opaque object in the path of the light beam, the transistor stops conducting current, and a logic 1 appears at the output. By feeding the output signal into a microcontroller and setting up interrupts on the rising edge of the signal, it is possible to measure the time between two pulses from the optocoupler.

The pulse at the output of the optocoupler indicates that the propeller of the motor has passed through the optocoupler. The time between pulses shows how long half a revolution of the motor around its axis lasts. Thus, the number of revolutions per minute (RPM) of the motor is calculated by the formula:

$$R = \frac{\frac{60}{2} * 10^6}{t_i}$$

where t_i is the time in microseconds between pulses. The obtained dependence of the motor acceleration is shown in Fig. 25. The initial and filtered signals are present on the graph. A moving average filter was used, with a window size of 7 points for the first 0.5 seconds and 40 points for subsequent time intervals.

The difference equation for a moving average filter looks as follows:

$$H(k) = \frac{1}{n} \sum_{i=k-n+1}^k x_i$$

Where n is the number of points for averaging.

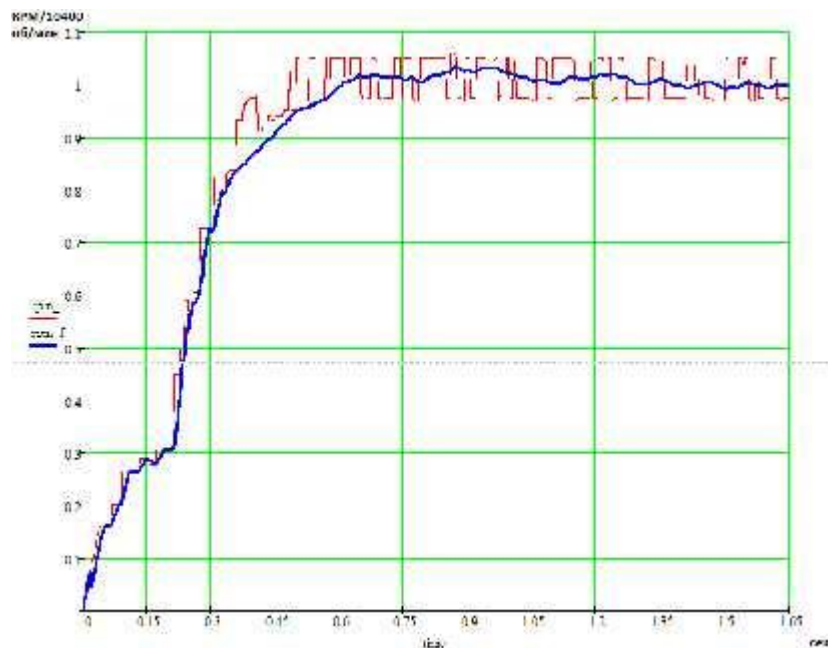


fig.19. The motor's response to the acceleration

Using the built-in identification tools in the Matlab package, we obtained the following transfer function of the motor:

$$W = \frac{K}{T * s + 1} = \frac{1.0491}{0.249 s + 1}$$

On Fig. 20, the window of the System Identification Toolbox is presented after the identification of the input data array.

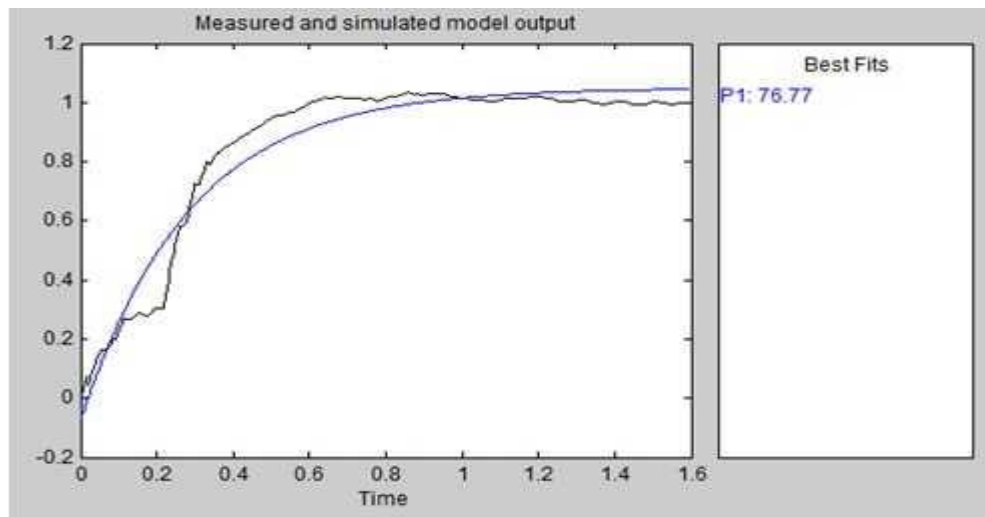


fig.20. System Identification Toolbox window

Thrust is proportional to the sum of the squares of the angular velocities of the propellers. The thrust coefficient needs to be calculated for the propeller rotation speed in hover mode.

Experimentally, it was found that the number of revolutions per minute at which the quadcopter takes off from the ground and maintains a given altitude is 4000 RPM. Let's convert this number to rad/s:

$$f = \frac{R * 2 \pi}{60} = 418.88$$

Then the thrust coefficient will be found using the formula:

$$b = \frac{m * g}{4 * f^2} = 0.96 * 1.3978 * 10^{-5} = 1.3418 * 10^{-5}$$

m is the mass of aircraft.

2.3.2 Moments of Inertia

Before starting to model the system, it is necessary to calculate the moments of inertia of the quadcopter relative to its axes, i.e., to fill in the inertia matrix.

For this we need to divide all aircraft to separate simple elements, formulas for calculating moments of inertia for which are known

So after dividing such elements were separated:

- 2 frame arms;
- 4 motors;
- 4 propellers;
- 1 battery;
- 1 Arduino Mega board;
- 1 bottom and 1 top frame plate.

To find the moment of inertia relative to the own axes of the aircraft, we use the theorem of parallel axis theorem (also known as the Huygens-Steiner theorem), which states: "The moment of inertia J of a body relative to any fixed axis equals the sum of the moment of inertia of Jc about the parallel axis passing through the center of mass of the body and the product of the body's mass m by the square of the distance d between the axes."

$$J = J_c + m * d^2$$

After weighing and measuring the dimensions of each highlighted part of the aircraft, the following table was filled, which contains a list of parts and their basic parameters necessary for calculating moments of inertia.

List of quadcopter parts

№	Part	Shape	Weight (kg)	Dimensions (m)	Distance to axis (m)
1	First and third frame arm	Parallelepiped	0.095	l=0.196 w=0.03 h=0.015	dx=0 dy=0.132 dz=0.132
2	Second and fourth frame arm	Parallelepiped	0.095	l=0.196 w=0.03 h=0.015	dx=0.132 dy=0 dz=0.132
3	Motor	Cylinder	0.06	r=0.01375 h=0.03	dx=0.02 dy=0.235 dz=0.235
4	Propeller	Cylinder	0.008	r=0.127 h=0.01	dx=0.05 dy=0.235 dz=0.235
5	Battery	Parallelepiped	0.179	l=0.102 w=0.034 h=0.022	dx=0.015 dy=0.015 dz=0
6	Arduino Mega	Parallelepiped	0.064	l=0.102 w=0.053	dx=0.01 dy=0.01

				h=0.01	dz=0
7	Upper frame plate	Thin plate	0.027	l=0.125 w=0.125	dx=0.005 dy=0.005 dz=0
8	Lower frame plate	Thin plate	0.038	l=0.18 w=0.125	dx=0.025 dy=0.025 dz=0
In	Total		0.96		

The frame arms, along with the speed controllers mounted along them, are parallelepipeds with lengths l , widths w , heights h , weights, and distances d from the center of gravity to the aircraft axes.

2.4 Modeling in Matlab

The dynamic model of the quadcopter in Simulink is shown in Figure 31. It utilizes the 6DOF block from the Aerospace Blockset library. The input parameters for the block are the forces acting on the quadcopter, namely gravity g , engine thrust T , and external torque M about the X, Y, and Z axes. The output parameters used in the model include the direction cosine matrix (DCM) for converting from the Earth coordinate system to the moving coordinate system of the aircraft, angular velocities p , q , and r , rotation angles ϕ , θ , and ψ in radians.

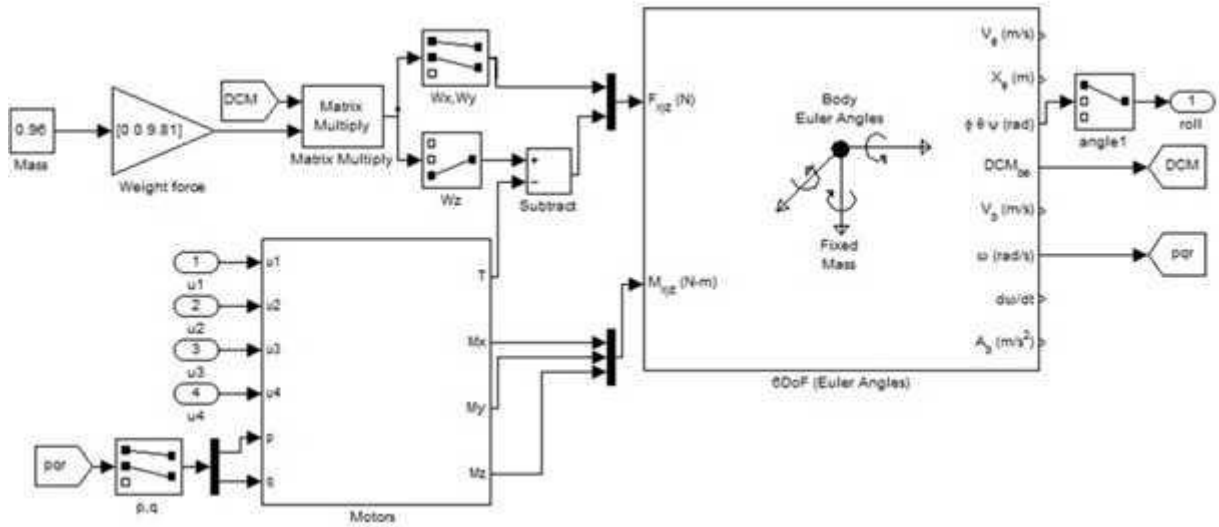


fig.21. quadcopter model in Simulink

Block 6DOF itself contains all the necessary motion equations derived earlier. Inside the block, you can set the initial conditions for position, the weight of the quadcopter, and the inertia tensor, as shown in Fig. 22.

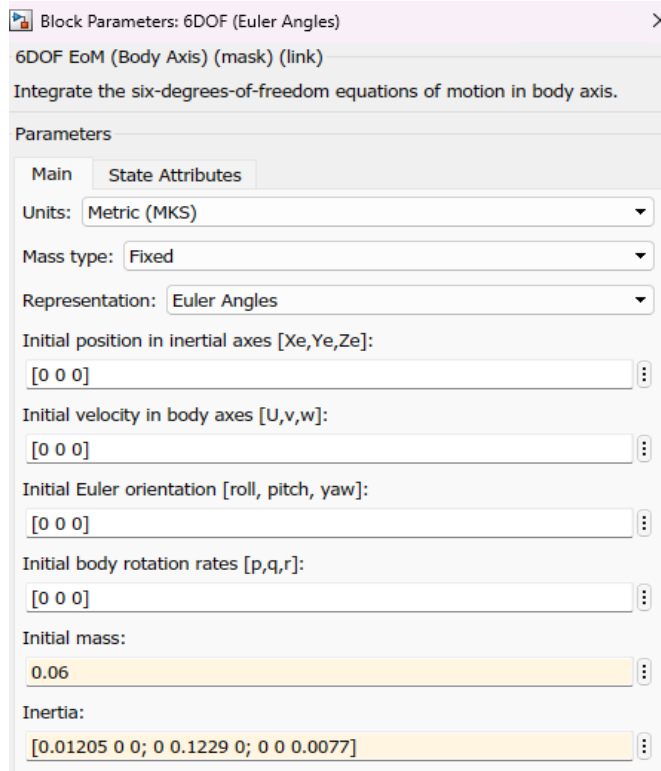


fig.22. 6DOF block settings

The Motors block (Fig. 23) simulates the behavior of the motors, with the input parameters being the speed of each of the four propellers in radians per second, and the angular velocities p , q , which add gyroscopic effects along the X and Y axes. The output parameters of the block are the rotational moments M and the thrust force T .

The sum of the squares of the propeller rotation speeds is multiplied by the thrust coefficient, thereby forming the thrust force T . Additionally, each pair of motors creates yaw moments M_x and M_y , which include gyroscopic effects G_x and G_y velocities. All four rotation speeds, multiplied by the coefficient of frontal resistance, form the yawing moment M_z .

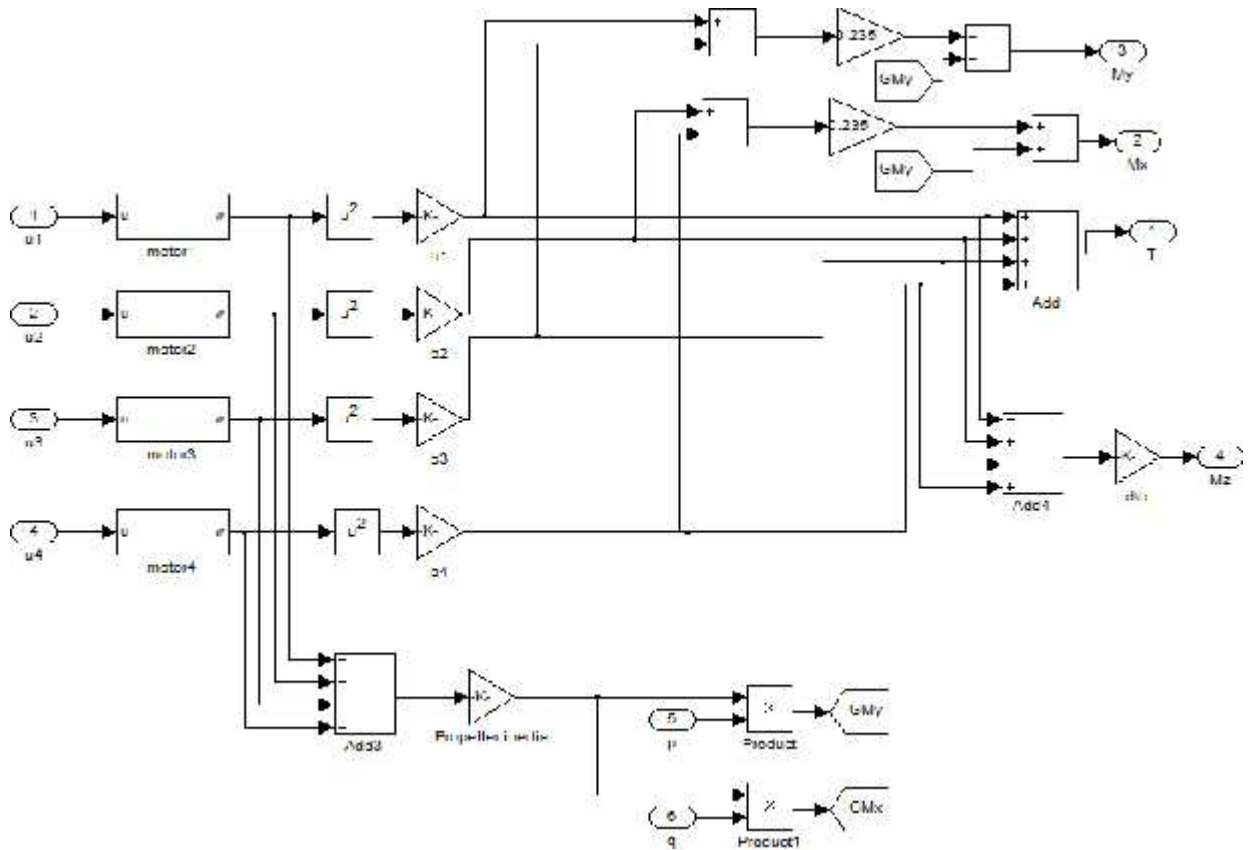


fig.23. Modeling the engines in Simulink

To stabilize the position of the aircraft, a PID controller was configured. For this purpose, the PID block with auto-tuning parameters was utilized. The output signal of the controller $u(t)$ is determined by three components:

$$u(t) = P + I + D = K_p * s(t) + K_i * \int_d^t s(r) * d + K_d * \left(\frac{a}{d}\right)$$

where K_p , K_i , and K_d are the proportional, integral, and derivative gain coefficients of the controller, respectively. The pitch angle stabilization scheme is shown in Fig.24. The initial engine speeds providing the quadcopter's hover mode are set to 420 rad/s.

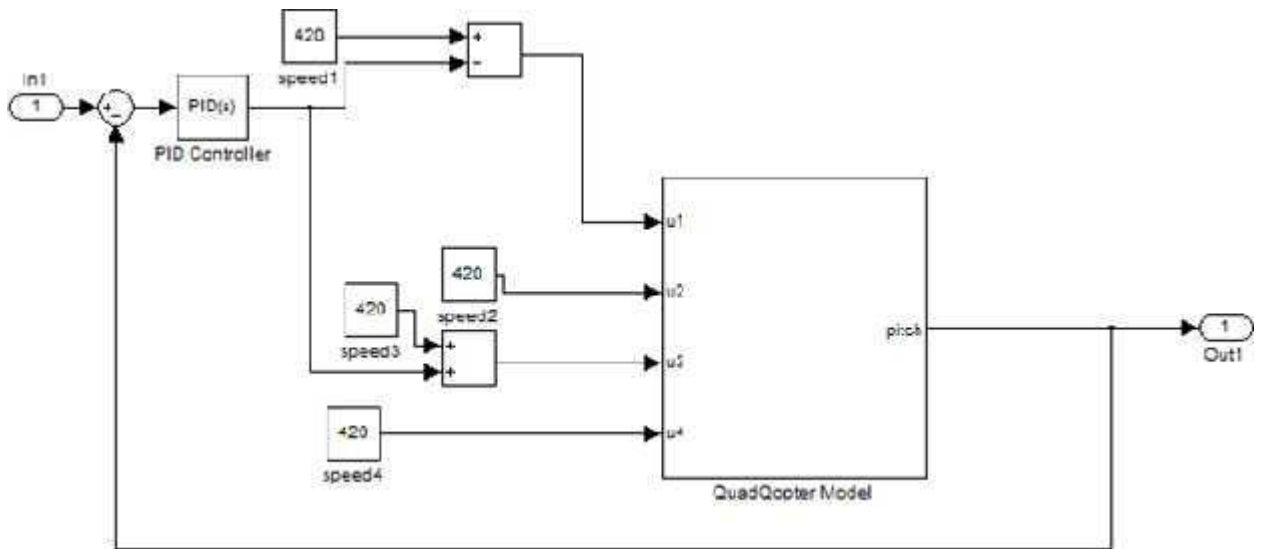


fig.24. Pitch angle stabilization using a PID controller

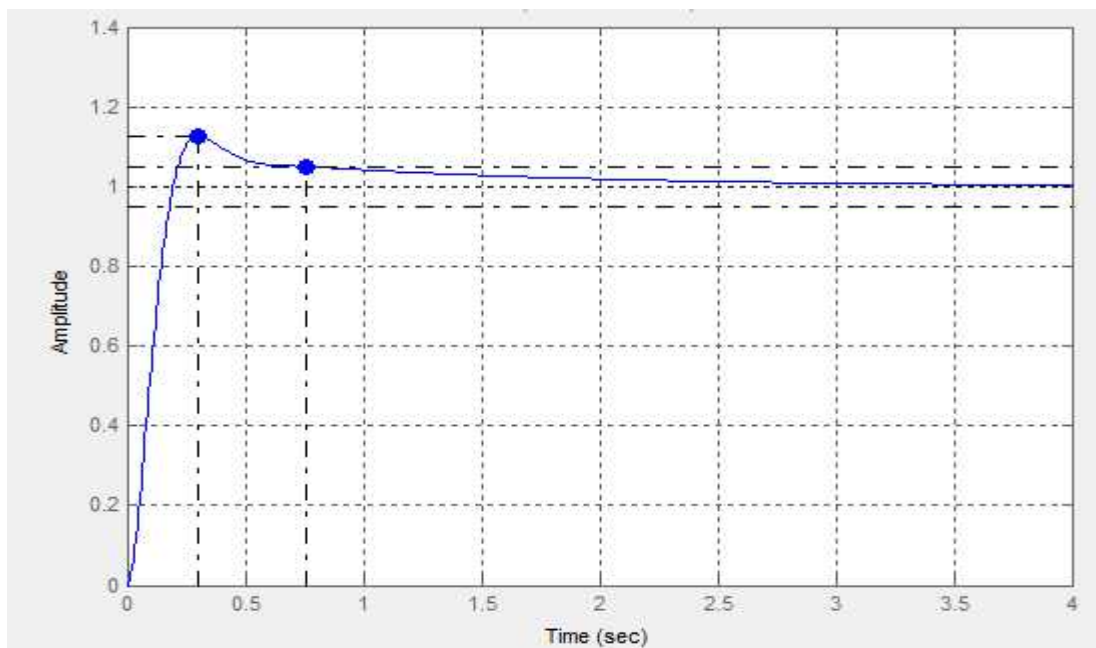


fig. 25. Step response for pitch angle

The same scheme is used for stabilizing the roll angle, only affecting engines number 2 and 4, respectively. Due to almost identical moments of inertia and graphs, we obtain nearly identical responses. The response to the input step change for the roll angle is shown in Figure 26.

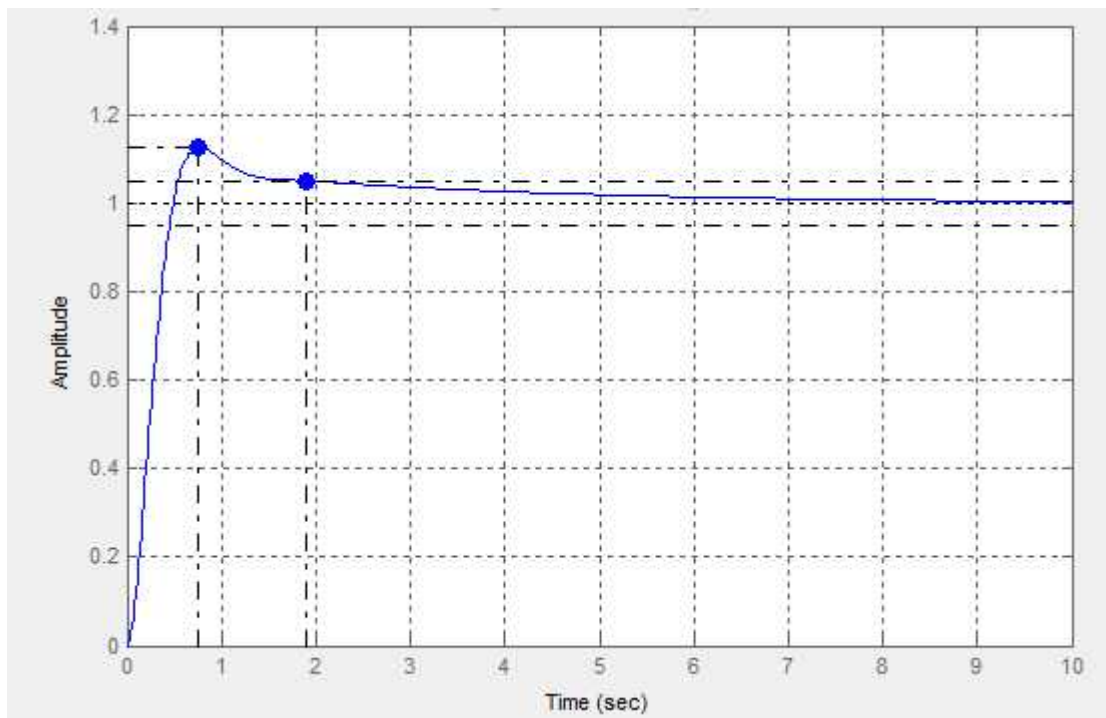


fig. 26. Response to a step input for the roll angle.

Having described the forces acting on the aircraft, we obtained equations of its motion, which represent the dependency of its angular coordinates on the forces acting on the aircraft, engine thrust, and technical characteristics. The resulting equations fully describe the behavior of the aircraft and serve as its mathematical model.

After identifying the individual elements of the aircraft: engines, thrust coefficient, and inertia matrix, a simulation was performed in Simulink to find the coefficients of the PID controller.

The found coefficients ensure good control quality, with the aircraft reaching the desired position within 1-2 seconds without significant overshoot.

Section 3

DETERMINING ORIENTATION IN SPACE

3.1 Magnetometer

A magnetometer is a device that measures the strength of the magnetic field along three mutually perpendicular axes - X, Y, Z, as shown in Figure 27.

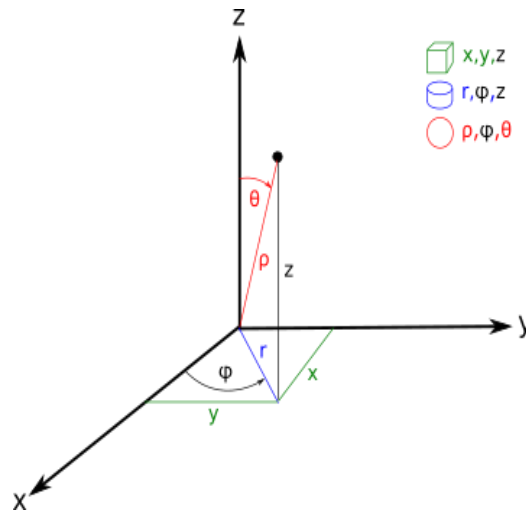


fig.27. The orientation of the magnetometer axes.

The direction and magnitude of the Earth's magnetic field are calculated from the voltage values of each axis of the magnetometer.

$$H_e = \sqrt{H_x^2 + H_y^2 + H_z^2}$$

As a typical application, the magnetometer is used as a compass, i.e., to determine the deviation in degrees from the north. Then it is assumed that the Z-component voltage, H, is zero, and the compass direction in degrees is determined by the formula:

$$H_e = \phi - \frac{180}{\pi} * a \quad \left| \frac{H_x}{H_y} \right|$$

$H_e=90$, if $H > 0$, and $H_e = 270$ if $H < 0$. In case $H = 0$, $H_e = 180$ (if $H_x < 0$) or $H_e = 0$ (if $H_x > 0$).

During the measurement of the magnetic field, errors may occur due to distortions in the magnetic field. There are two main reasons for this:

- Hard distortion: displacement of the measured magnetic field of the Earth due to the presence of objects with their own magnetic field nearby.
- Soft distortion: distortion of the existing magnetic field due to the presence of metals arranged nearby, such as nickel or iron.

Figure 28 shows the rotation around the Z-axis of the magnetometer, which does not encounter any obstacles.

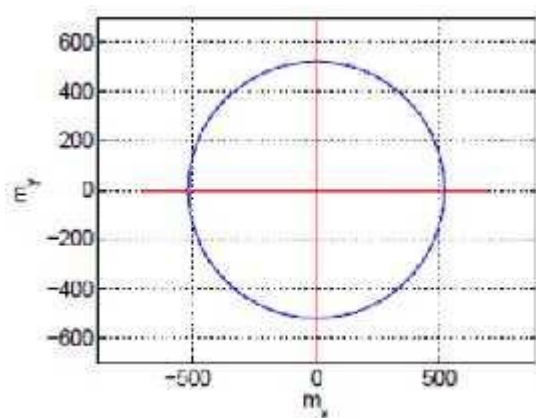


fig.28 Ideal measurement of the magnetic field

The presence of devices or instruments around the magnetometer that cause hard distortion contains the center of the circle, is shown on Figure 29.

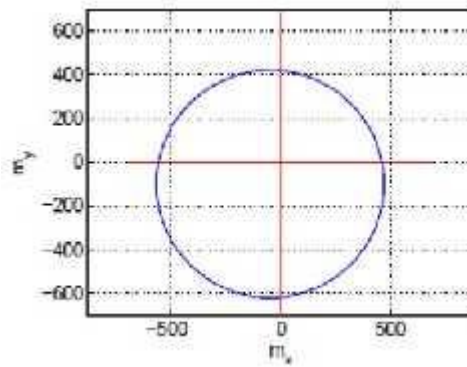


fig. 29. Presence of hard distortion of the magnetic field

Simultaneous presence of hard and soft distortions will not only shift the circle's center but also elongate it into an ellipse, as shown in Figure 30.

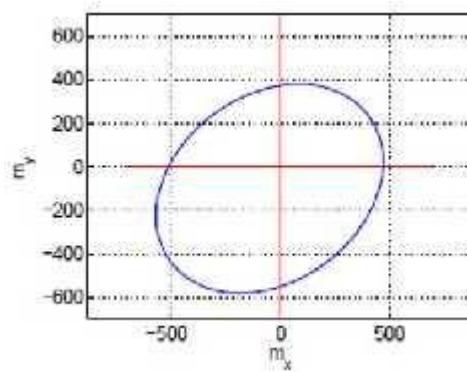


fig. 30. Simultaneous presence of hard and soft magnetic field distortions

To eliminate the mentioned distortions, it is sufficient to attempt to remove their source from the area of measurement of the magnetic field. However, if this is not possible, the following model will be used, which allows for distortion compensation:

$$M = \begin{bmatrix} C1 & C2 & C3 \\ C4 & C5 & C6 \\ C7 & C8 & C9 \end{bmatrix} \begin{bmatrix} H_x \\ H_y \\ H_z \end{bmatrix} + \begin{bmatrix} -C10 \\ C11 \\ -C12 \end{bmatrix}$$

The first matrix is called the transformation matrix and consists of numerous parameters i , which are aimed at compensating for soft distortions, while the second one is the offset matrix,

allowing to shift the circle center to the origin of the coordinates, thus compensating for hard distortions.

In some cases, measurement errors are caused by the misalignment of the sensor's internal axes and their different sensitivities. To correct this, a sensor calibration procedure is required. The result of calibration will be the found transformation and offset matrices.

To perform magnetometer calibration, it is mounted in a way that allows it to be easily rotated around an axis. The sensor is connected to an Arduino via the I2C protocol and transmits data to the computer at a specified interval, for example, every 200 ms. By rotating the sensor in the horizontal plane by 360 degrees, the magnetic induction vector will trace a circle on an imaginary sphere (see Figure 31).

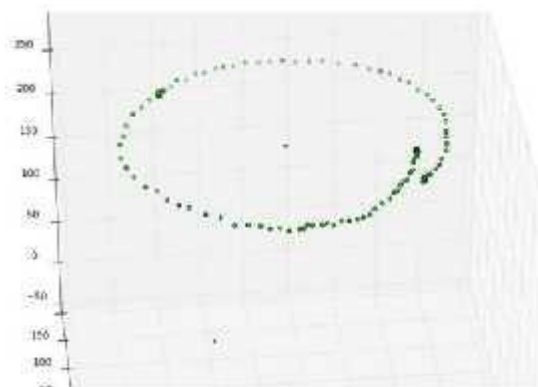


fig.31 The values of the magnetic induction vector during a full rotation.

By flipping the sensor to the opposite side and then rotating it again by 360 degrees, we obtain another circle on the sphere around the gravity vector. Connecting the centers of these circles gives us a line parallel to one of the sensor's axes. By measuring the deviation from this line, we can determine the correction needed.

The algorithm for obtaining the transformation matrix is as follows:

1. For each side of the sensor, record the coordinates of two points, A and B. The second point is found by rotating the sensor 180 degrees from its initial position.

$$\overline{P_{i1} = (X, Y, Z), P_{i2} = (X, Y, Z)}$$

2. Find the centers of rotation circles using two points for each side:

$$P_{c1} = \frac{P_{i1} + P_{i2}}{2}$$

3. Connect the opposite centers, thereby obtaining the relative orientation of the sensor axes (see Figure 32).

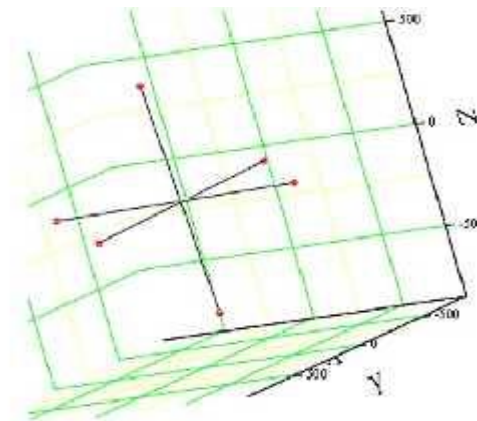


Fig. 32. Relative orientation of axes of an uncalibrated sensor

4. Subtract opposite vectors from each other to obtain a set of vectors indicating the actual relative orientation of the axes. The axis corresponding to each such vector is indicated by the same significant element.

5. Divide each vector by its most significant element, resulting in a 3x3 column matrix.

6. The inverse of this matrix is the transformation matrix.

Determination of the displacement matrix:

1. Find the centers of three lines formed by connecting two opposite circle centers.

$$X_C = \frac{P_C + P_C}{2}$$

2. The displacement matrix B is calculated by the formula:

$$B = \frac{X_{C1} + X_{C2} + X_{C3}}{3}$$

The calibration result is presented in Figure 33. Using the obtained matrices, calibrated voltage vector values are calculated in real-time on the microcontroller, allowing to eliminate magnetic distortions and non-perpendicularity of internal axes.

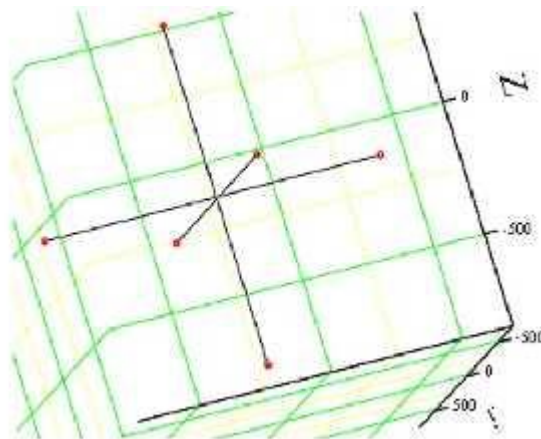


fig. 33. Sensor axis alignment after calibration

3.2 Accelerometer and Gyroscope

The accelerometer measures the projections of acceleration along its axes. Using the formulas described below, you can find the roll and pitch angles, but accelerometer data always contain a large amount of noise, as the accelerometer itself is very sensitive even to minor vibrations. Therefore, to determine the orientation, the gyroscope is used in conjunction with the accelerometer.

$$\phi = \text{atan}\left(\frac{a_y}{a_z}\right)$$

$$\theta = \text{asin}\left(\frac{a_x}{g}\right)$$

where a_x , a_y , and a_z are the accelerometer data along its axes, and g is the acceleration due to gravity. The gyroscope measures angular velocities around its axes. By integrating the gyroscope data over time, we obtain the rotation angles around the axes.

$$\phi = \int_0^t r(r) dr$$

Або використовуючи різницеве рівняння:

$$\phi[n] - \phi[n, 1] \Big|_{h * r}$$

where h is the time between data samples

r is the value of angular velocity.

3.3 Joint use of gyroscope and magnetometer

When using only the gyroscope to determine orientation, even when compensating its data with the accelerometer, a significant drift around the Z-axis is observed.

To determine the yaw angle, it is necessary to use the magnetometer readings. Using the provided formulas, the calculated data will be correct only if the magnetometer is parallel to the Earth's surface, meaning it has no angles of inclination around its X and Y axes. To obtain accurate data from the magnetometer, regardless of its tilt angle, it is necessary to make the corresponding correction to the magnetometer's value at each tilt angle.

This method insufficiently compensates for tilt angles, significantly affecting accuracy, and furthermore, when operating with Euler angles, there is always a likelihood of ambiguity or gimbal lock, where two axes coincide in determining the rotation sequence.

One method to prevent gimbal lock is to use quaternions instead of Euler angles in the magnetometer compensation stage. Quaternions are four-component vectors that describe rotation around an axis by a 0 angle, thus specifying the orientation of an object in space.

3.4 Madgwick Filter

One of the most popular algorithms for determining orientation, i.e., obtaining accurate pitch, yaw, and roll angles, was developed by Sebastian Madgwick in 2011.

In his work, a detailed description of the filter is provided, including its implementation in C++. The filter utilizes quaternions, allowing the involvement of accelerometer and magnetometer data for analytical calculations, as well as for the correction of gyroscope drift in the form of quaternion derivatives using gradient descent optimization.

The author presents experimental results demonstrating that the accuracy level of the developed filter exceeds that of a Kalman filter-based one:

- No more than 0.6 RMS deviation in stationary state.
- No more than 0.8 RMS deviation in motion state.

Advantages of the Madgwick filter include:

- Low computational resources required: 277 simple arithmetic operations per filter update.
- Effectiveness at low sampling rates (e.g., 10 Hz).

3.5 FreeIMU Library

For the platform used in this project, there exists the FreeIMU library, developed by Fabio Varesano as part of his dissertation. This library contains all the necessary functions for interacting with the GY-88 position sensor and enables obtaining information about rotation angles using the Madgwick filter.

Additionally, there is software available for calibrating the magnetometer and accelerometer sensors (see Figure 34).

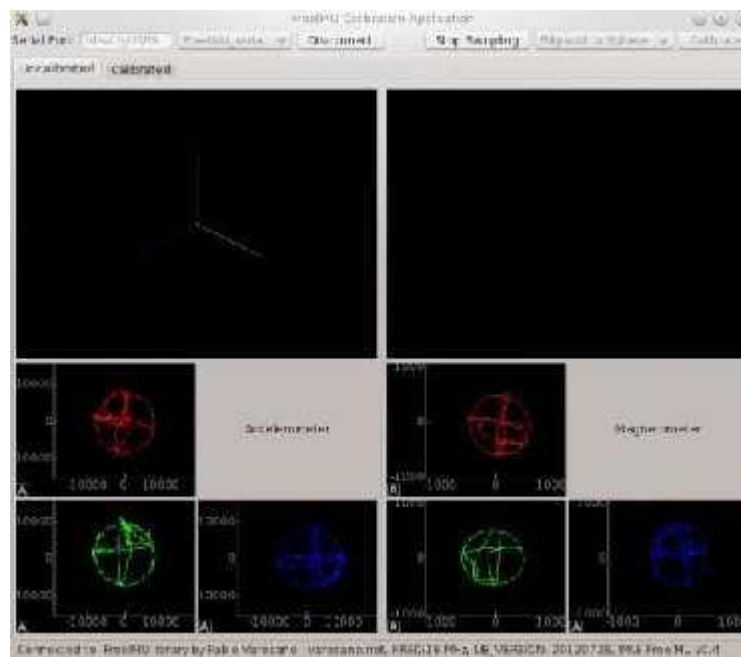


fig.34 FreeIMU Application Window for Sensor Calibration

This library will be used in writing the main program for controlling the quadcopter in this project. 3.6 Using the Moving Average Filter To determine the current roll, pitch, and yaw

angles, the FreeIMU library with the built-in implementation of the Madgwick filter is used in

the project.

However, in practice, the obtained roll and pitch angles were not stable and had constant spikes of 0.75. Therefore, a decision was made to filter the data obtained from FreeIMU. With a 15-point averaging, the filter shows acceptable results, introducing a slight but not critical delay when changing the actual position of the aircraft (see figures 35-36).

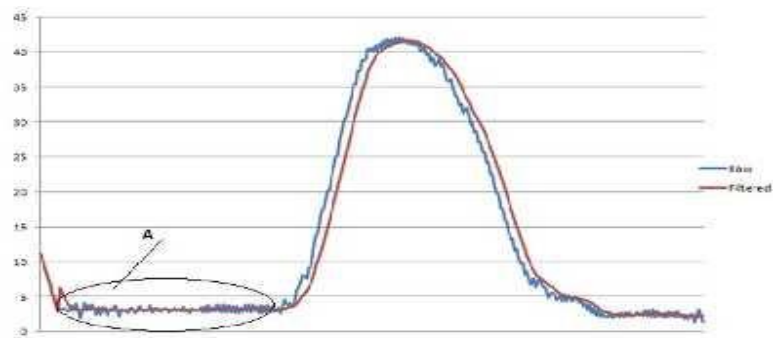


fig 35. Raw and filtered pitch angle data

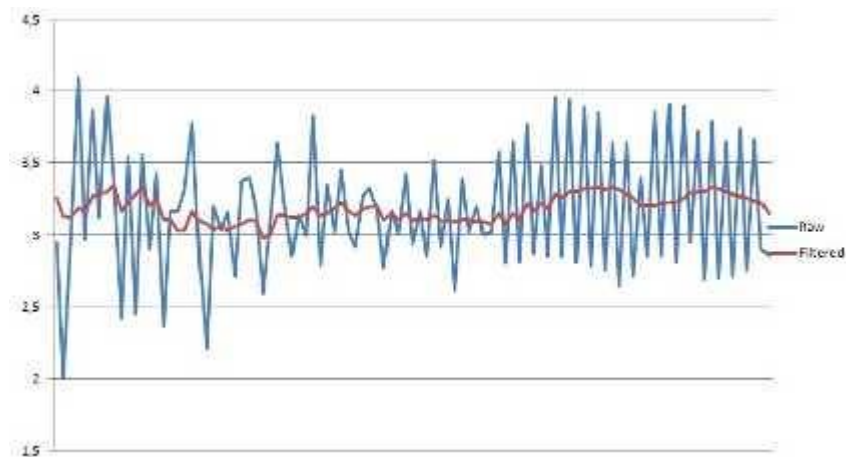


Figure 36. Pitch angle change data

Section 4

AUTOMATIC CONTROL SYSTEM OF THE AIRCRAFT

The controlling microcontroller Arduino Mega 2560 serves as the central hub of the system. Interfacing via the two-wire I2C interface with the gyroscope, accelerometer, and magnetometer sensors, which are part of the GY module and act as a feedback loop for position stabilization, the microcontroller gains an understanding of the UAV's coordinates in space.

After obtaining the necessary coordinates, the microcontroller generates control interaction in the form of Pulse Width Modulation (PWM) pulses to the speed controllers to increase or decrease the rotation speed of specified motors, leading to the adjustment of the UAV's orientation.

To generate PWM pulses of the required duration, the microcontroller's digital outputs are used along with one of its built-in 16-bit timers, allowing the setting of necessary pulse duration boundaries from 1000 (minimum speed) to 2000 (maximum speed) microseconds, suitable for most speed controllers.

The drone is remotely controlled in the remote mode using a transmitter capable of transmitting seven different control signals within a single PWM wave. For the given task, four channels were required (see Figure 48):

- Channel 1: Roll angle adjustment;
- Channel 3: Pitch angle control;
- Channel 4: Yaw angle control;
- Channel 2: Altitude control.



Figure 38. Graphical representation of the PWM signal transmitting signals from four control channels in a single packet.

The PWM signal, upon reaching the receiver, is decomposed into seven Pulse Width Modulation (PWM) signals for each control channel. Digital inputs of the microcontroller configured for external interrupts on rising and falling edges were used to obtain the PWM signal values. Interrupts are events that require the current program execution to halt and call an interrupt handler, after which the program resumes its execution. In the interrupt handlers, the current start time of the event was recorded, and by finding the time difference between the rising and falling edges, the pulse duration of the signals coming from the PWM receiver was determined. The pulse duration, like in PWM signals, varies from 1000 to 2000 microseconds.

The block diagram of the main program algorithm is presented in Figure 39.

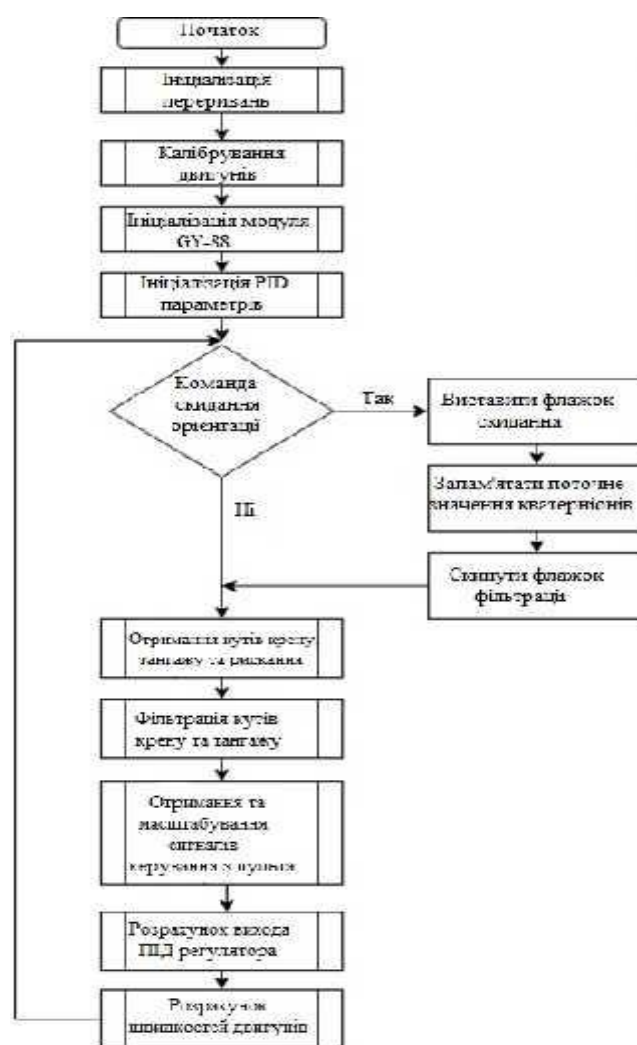


fig.39 diagram of program

At the beginning of the infinite loop, there is a check for resetting the orientation of the aircraft. If channels 1, 2, and 3 simultaneously transmit values less than 1100 from the remote control, then the reset flag is set. This flag is used in calculating the angles from quaternions. The current quaternion value is memorized, and the filtering flag is discarded, allowing the program filter to restart. Thus, in the current position of the aircraft, its orientation angles become zero.

The procedure for obtaining orientation angles calculates the roll, pitch, and yaw angles using the formula described above in the calculations in section 3.4. Moreover, if the orientation reset flag was set, then each quaternion component is recalculated as follows:

where q_{new} - current quaternion value at the time of reset, q_{old} - current quaternion value.

The part of the program responsible for receiving and scaling signals from the control remote sets the following control signal ranges:

- Throttle: 0-70%
- Roll control: -20-20
- Pitch control: -20-20
- Yaw control: 180-180

All signals except for throttle are inputs for calculating the control influence of the PID regulator for the corresponding angle. Engine power is determined by the throttle, which defines the ascent rate of the quadcopter. The throttle is limited to 70% of the possible engine power. The remaining 30% is used for stabilizing the aircraft.

As a result of tests conducted on real objects, it was decided to change the coefficients of the PID regulator found during modeling for better system stabilization.

The change in coefficients was prompted by simplifications made during model development, but primarily due to one of the engines being found less powerful and less responsive than the others during experiments.

The conclusion drawn from the work performed is that to create an automatic stabilization system for the aircraft, it is necessary to obtain its mathematical model and perform identification of the unknown parameters involved in the model. The results obtained from modeling to find the control law for the aircraft are acceptable both for simulation purposes and for the final control object. However, for a more quality regulation process, manual tuning of the PID controller parameters may be necessary.

It was also found that the use of intelligent sensors along with software filtering algorithms allows for obtaining reliable information about the aircraft's position in space.